
Learning Energy-based Model with Flow-based Backbone by Neural Transport MCMC

Erik Nijkamp*
UCLA
enijkamp@ucla.edu

Ruiqi Gao*
UCLA
ruiqigao@ucla.edu

Pavel Sountsov
Google
siege@google.com

Srinivas Vasudevan
Google
srvasude@google.com

Bo Pang
UCLA
bopang@ucla.edu

Song-Chun Zhu
UCLA
sczhu@stat.ucla.edu

Ying Nian Wu
UCLA
ywu@stat.ucla.edu

Abstract

Learning energy-based model (EBM) requires MCMC sampling of the learned model as the inner loop of the learning algorithm. However, MCMC sampling of EBM in data space is generally not mixing, because the energy function, which is usually parametrized by deep network, is highly multi-modal in the data space. This is a serious handicap for both the theory and practice of EBM. In this paper, we propose to learn EBM with a flow-based model serving as a backbone, so that the EBM is a correction or an exponential tilting of the flow-based model. We show that the model has a particularly simple form in the space of the latent variables of the flow-based model, and MCMC sampling of the EBM in the latent space, which is a simple special case of neural transport MCMC, mixes well and traverses modes in the data space. This enables proper sampling and learning of EBM.

1 Introduction

The energy-based model (EBM) [40, 46, 27, 58, 57, 13, 36, 47, 11, 12] defines an unnormalized probability density function on the observed data such as images via an energy function, so that the density is proportional to the exponential of the negative energy. Taking advantage of the approximation capacity of modern deep networks such as convolutional network (ConvNet) [39, 34], recent papers [57, 13, 36, 47, 11] parametrize the energy function by ConvNet. The ConvNet-EBM is highly expressive and the learned EBM can produce realistic synthesized examples.

The EBM can be learned by maximum likelihood, and the gradient-based maximum likelihood learning algorithm follows an “analysis by synthesis” scheme. In the synthesis step, synthesized examples are generated by sampling from the current model. In the analysis step, the model parameters are updated based on the statistical difference between synthesized examples and observed examples. The synthesis step usually requires Markov chain Monte Carlo (MCMC) sampling, and gradient-based sampling such as Langevin dynamics [37] or Hamiltonian Monte Carlo (HMC) [44] can be conveniently implemented on the current deep learning platforms where gradients can be efficiently and automatically computed by back-propagation.

*Equal contribution.

However, gradient-based MCMC sampling in the data space generally does not mix. The data distribution is typically highly multi-modal. To approximate such a distribution, the density function or the energy function of the ConvNet-EBM needs to be highly multi-modal as well. When sampling from such a multi-modal density in the data space, gradient-based MCMC tends to get trapped in local modes with little chance to traverse the modes freely, rendering the MCMC non-mixing. Without being able to generate fair examples from the model, the estimated gradient of the maximum likelihood learning can be very biased, and the learned model can be far from the maximum likelihood estimate (MLE). Even if we can learn the model by other means without resorting to MCMC sampling, e.g., by noise contrastive estimation (NCE) [19, 14], it is still necessary to be able to draw fair examples from the learned model for the purpose of model checking or some downstream applications based on the learned model.

Accepting the fact that MCMC sampling is not mixing, contrastive divergence [52] initializes finite step MCMC from the observed examples, so that the learned model is admittedly biased from the MLE. Recently, [47] proposes to initialize short-run MCMC from a fixed noise distribution, and shows that even though the learned EBM is biased, the short-run MCMC can be considered a valid model that can generate realistic examples. This partially explains why EBM learning algorithm can synthesize high quality examples even though the MCMC does not mix. However, the problem of non-mixing MCMC remains unsolved. Without proper MCMC sampling, the theory and practice of learning EBM is on a very shaky ground. The goal of this paper is to address this problem.

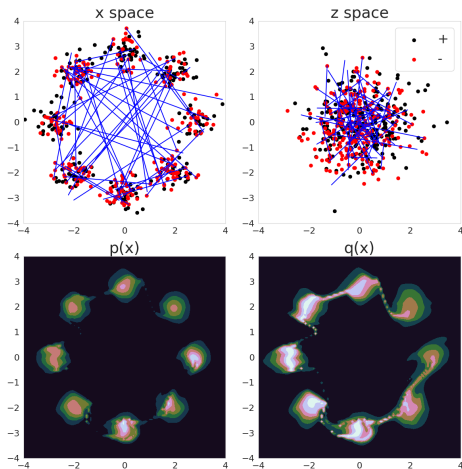


Figure 1: Demonstration of the mixing MCMC with neural transport on a mixture of Gaussians as target distribution. *Top*: Trajectories of Markov chains in data space x and latent space z . *Bottom*: Density estimations with exponentially tilted model p_θ of underlying flow q_α .

We propose to learn the EBM with a flow-based model as a backbone model, so that the EBM is in the form of a correction, or an exponential tilting, of the flow-based model. Flow-based models have gained popularity in generative modeling [9, 10, 31, 18, 3, 35, 53] and variational inference [30, 49, 32, 28, 26]. Similar to the generator model [30, 17], flow-based model is based on a mapping from latent space to the data space. However, unlike the generator model, the mapping in the flow-based model is one-to-one, with closed form inversion and Jacobian. This leads to an explicit normalized density via change of variable. However, to ensure tractable inversion and Jacobian, the mapping in the flow-based model has to be a composition of a sequence of simple transformations of highly constrained forms. In order to approximate a complex distribution, it is necessary to compose a large number of such transformations. In our work, we propose to learn EBM by correcting a relatively simple flow-based model with a relatively simple energy function parametrized by a free-form ConvNet. We show that the resulting EBM has a particularly simple form in the space of the latent variables of the flow-based model. MCMC sampling of the EBM in the latent space, which is a simple special case of neural transport MCMC [24], mixes well and is able to traverse modes in the data space. This enables proper sampling and learning of EBM.

Our experiments show that it is possible to learn EBM with flow-based backbone, and the neural transport sampling of the learned EBM solves or greatly mitigates the non-mixing problem of MCMC.

2 Contributions and related work

Contributions. This paper tackles the problem of non-mixing of MCMC for sampling from an EBM. We propose to learn EBM with a flow-based backbone model. The resulting EBM in the latent space is of a simple form that is much more friendly to MCMC mixing.

The following are research themes in generative modeling and MCMC sampling that are closely related to our work.

Neural transport MCMC. Our work is inspired by neural transport sampling [24]. For an unnormalized target distribution, the neural transport sampler trains a flow-based model as a variational approximation to the target distribution, and then samples the target distribution in the space of latent variables of the flow-based model via change of variable. In the latent space, the target distribution is close to the prior distribution of the latent variables of the flow-based model, which is usually a unimodal Gaussian white noise distribution. Consequently the target distribution in the latent space is close to be unimodal and is much more conducive to the mixing and fast convergence of MCMC than sampling in the original space [43].

Our work is a simplified special case of this idea, where we learn the EBM as a correction of a pre-trained flow-based model, so that we do not need to train a separate flow-based approximation to the EBM. The energy function, which is a correction of the flow-based model, does not need to reproduce the content of the flow-based model, and thus can be kept relatively simple. Moreover, in the latent space, the resulting EBM takes on a very simple form where the inversion and Jacobian in the flow-based model disappear. This may allow for more free-form flow-based model where inversion and Jacobian do not need to be in closed form [18, 3].

Energy-based corrections. Our model is based on an energy-based correction or an exponential tilting of a more tractable model. This idea has been explored in noise contrastive estimation (NCE) [19, 14] and introspective neural networks (INN) [54, 25, 38], where the correction is obtained by discriminative learning. Earlier works include [50, 56]. Correcting or refining a simpler and more tractable backbone model can be much easier than learning an EBM from scratch, because the EBM does not need to reproduce the knowledge learned by the backbone model. It also allows easier sampling of EBM.

Latent space sampling. Non-mixing MCMC sampling of an EBM is a clear call for latent variables to represent multiple modes of the original model distribution via explicit top-down mapping, so that the distribution of the latent variables is less multi-modal. Earlier work in this direction include [4, 6, 36]. In this paper, we choose to use flow-based model for its simplicity, because the distribution in the data space can be translated into the distribution in the latent space by a simple change of variable, without requiring integrating out extra dimensions as in the generator model.

3 Model and learning

3.1 Flow-based model

Let x be the input example, such as an image. A flow-based model is of the form

$$z \sim q_0(z), \quad x = g_\alpha(z), \tag{1}$$

where z is the latent vector of the same dimensionality as x , and q_0 is a known prior distribution such as Gaussian white noise distribution. g_α is a composition of a sequence of invertible transformations whose inversion and log-determinants of the Jacobians can be obtained in closed form. As a result, these transformations are of highly constrained forms. α denotes the parameters. Let $q_\alpha(x)$ be the probability density at x under the transformation $x = g_\alpha(z)$, then according to the change of variable,

$$q_0(z)dz = q_\alpha(x)dx, \tag{2}$$

where dz and dx are understood as the volumes of the infinitesimal local neighborhoods around z and x respectively under the mapping $x = g_\alpha(z)$. Then for a given x , $z = g_\alpha^{-1}(x)$, and

$$q_\alpha(x) = q_0(z)dz/dx = q_0(g_\alpha^{-1}(x))|\det(\partial g_\alpha^{-1}(x)/\partial x)|, \tag{3}$$

where the ratio between the volumes dz/dx is the absolute value of the determinant of the Jacobian.

Suppose we observe training examples $(x_i, i = 1, \dots, n) \sim p_{\text{data}}(x)$, where p_{data} is the data distribution, which is typically highly multi-modal. We can learn α by MLE. For large n , the MLE of α minimizes the Kullback-Leibler divergence $D_{KL}(p_{\text{data}}||q_\alpha)$. q_α strives to cover most of the modes in p_{data} , and the learned q_α tends to be more dispersed than p_{data} . In order for q_α to approximate p_{data} closely, it is usually necessary for g to be a composition of a large number of transformations of highly constrained forms with closed-form inversions and Jacobians. The learned mapping $g_\alpha(z)$ transports the unimodal Gaussian white noise distribution to a highly multi-modal distribution q_α in the data space as an approximation to the data distribution p_{data} .

3.2 Energy-based model

An energy-based model (EBM) is defined as follows:

$$p_\theta(x) = \frac{1}{Z(\theta)} \exp(f_\theta(x))q(x), \quad (4)$$

where $q(x)$ is a reference measure, such as the uniform measure or a Gaussian white noise distribution as in [57]. f_θ is defined by a bottom-up ConvNet whose parameters are denoted by θ . The normalizing constant or the partition function $Z(\theta) = \int \exp(f_\theta(x))q(x)dx = \mathbb{E}_q[\exp(f_\theta(x))]$ is typically analytically intractable.

Suppose we observe training examples $x_i \sim p_{\text{data}}$ for $i = 1, \dots, n$. For large n , the sample average over $\{x_i\}$ approximates the expectation with respect to p_{data} . For notational convenience, we treat the sample average and the expectation as the same.

The log-likelihood is

$$L(\theta) = \frac{1}{n} \sum_{i=1}^n \log p_\theta(x_i) \doteq \mathbb{E}_{p_{\text{data}}}[\log p_\theta(x)]. \quad (5)$$

The derivative of the log-likelihood is

$$L'(\theta) = \mathbb{E}_{p_{\text{data}}}[\nabla_\theta f_\theta(x)] - \mathbb{E}_{p_\theta}[\nabla_\theta f_\theta(x)] \doteq \frac{1}{n} \sum_{i=1}^n \nabla_\theta f_\theta(x_i) - \frac{1}{n} \sum_{i=1}^n \nabla_\theta f_\theta(x_i^-), \quad (6)$$

where $x_i^- \sim p_\theta(x)$ for $i = 1, \dots, n$ are synthesized examples sampled from the current model $p_\theta(x)$.

The above equation leads to the ‘‘analysis by synthesis’’ learning algorithm. At iteration t , let θ_t be the current model parameters. We generate $x_i^- \sim p_{\theta_t}(x)$ for $i = 1, \dots, n$. Then we update $\theta_{t+1} = \theta_t + \eta_t L'(\theta_t)$, where η_t is the learning rate.

To generate synthesized examples from p_θ , we can use gradient-based MCMC sampling such as Langevin dynamics [37] or Hamiltonian Monte Carlo (HMC) [44], where $\nabla_x f_\theta(x)$ can be automatically computed. Since p_{data} is in general highly multi-modal, the learned p_θ or f_θ tends to be multi-modal as well. As a result, gradient-based MCMC tends to get trapped in the local modes of f_θ with little chance of mixing between the modes.

3.3 Energy-based model with flow-based backbone

Instead of using uniform or Gaussian white noise distribution for the reference distribution $q(x)$ in the EBM in (4), we can use a relatively simple flow-based model q_α as the reference model. q_α can be pre-trained by MLE, and serves as the backbone of the model, so that the model is of the following form

$$p_\theta(x) = \frac{1}{Z(\theta)} \exp(f_\theta(x))q_\alpha(x), \quad (7)$$

which is almost the same as in (4) except that the reference distribution $q(x)$ is a pre-trained flow-based model $q_\alpha(x)$. The resulting model $p_\theta(x)$ is a correction or refinement of q_α , or an exponential tilting of $q_\alpha(x)$, and $f_\theta(x)$ is a free-form ConvNet to parametrize the correction. The overall negative energy is $f_\theta(x) + \log q_\alpha(x)$.

In the latent space of z , let $p(z)$ be the distribution of z under $p_\theta(x)$, then

$$p(z)dz = p_\theta(x)dx = \frac{1}{Z(\theta)} \exp(f_\theta(x))q_\alpha(x)dx. \quad (8)$$

Recall equation (2), $q_\alpha(x)dx = q_0(z)dz$, we have

$$p(z) = \frac{1}{Z(\theta)} \exp(f_\theta(g_\alpha(z)))q_0(z). \quad (9)$$

$p(z)$ is an exponential tilting of the prior noise distribution $q_0(z)$. It is a very simple form that does not involve the Jacobian or inversion of $g_\alpha(z)$.

We can also apply the above exponential tilting and change of variable scheme to the generator model, i.e., using the generator model as the backbone model. However, for the generator model, $q(x)$ is not in closed form, and after exponential tilting, the marginal $p(z)$ requires integral. See Appendix 6.2 for details. In comparison, flow-based model is simpler and more explicit.

3.4 Learning by Hamiltonian neural transport sampling

Instead of sampling $p_\theta(x)$, we can sample $p(z)$ in (9). While $q_\alpha(x)$ is multi-modal, $q_0(z)$ is unimodal. Since $f_\theta(x)$ is a correction of q_α , $p(z)$ is a correction of $p_0(z)$, and can be much less multi-modal than $p_\theta(x)$ in the data space. After sampling z from $p(z)$, we can generate $x = g_\alpha(z)$.

The above MCMC sampling scheme is a special case of neutral transport MCMC proposed by [24] for sampling from an EBM or the posterior distribution of a generative model. The basic idea is to train a flow-based model as a variational approximation to the target EBM, and sample the EBM in the latent space of the flow-based model. In our case, since p_θ is a correction of q_α , we can simply use q_α directly as the approximate flow-based model in neural transport sampler. The extra benefit is that the distribution $p(z)$ is of an even simpler form than $p_\theta(x)$, because $p(z)$ does not involve the inversion and Jacobian of g_α . As a result, we may use a flow-based backbone model of a more free form such as one based on residual network [3], and we will leave this issue to future investigation.

We use Hamiltonian Monte Carlo (HMC) [44] to sample from $p(z)$. We can then learn θ by MLE according to equation (6). Algorithm 1 describes the detailed learning algorithm. We refer to Appendix 6.4 for details.

Algorithm 1: Learning the correction f_θ with Hamiltonian neural transport (NT).

input : Learning iterations T , learning rate η , batch size m , pre-trained parameters α , initial parameters θ_0 , initial latent variables $\{z_{i,0}\}_{i=1}^m \sim q_0(z)$, observed examples $\{x_i\}_{i=1}^n$, number of MCMC steps K in each learning iteration.

output : Parameters $\{\theta_T\}$.

for $t = 0 : T - 1$ **do**

1. Update $\{z_{i,t}\}_{i=1}^m$ by HMC with target distribution $p(z)$ in equation (9) for K steps.
 2. Push the z -space samples forward through g_α to obtain synthesized examples $\{x_i^-\}_{i=1}^m$.
 3. Draw observed training examples $\{x_i\}_{i=1}^m$.
 4. Update θ according to (6).
-

3.5 Learning by noise contrastive estimation

We may also learn the correction $f_\theta(x)$ discriminatively, as in noise contrastive estimation (NCE) [19] or introspective neural networks (INN) [54, 25, 38]. Let x_i^+ , $i = 1, \dots, n$ be the training examples, which are treated as positive examples, and let x_i^- , $i = 1, \dots, n^-$ be the examples generated from $q_\alpha(x)$, which are treated as negative examples. For each batch, let ρ be the proportion of positive examples, and $1 - \rho$ the proportion of negative examples. Then

$$\log[P(+|x)/P(-|x)] = \log[\rho/(1 - \rho)] - \log Z(\theta) + f_\theta(x) = b + f_\theta(x), \quad (10)$$

where $b = \log[\rho/(1 - \rho)] - \log Z(\theta)$ is treated as a separate bias parameter. Then we can estimate b and θ by fitting a logistic regression on the positive and negative examples.

Note, that NCE is the discriminator side of GAN. Similar to GAN, we can also improve the flow-based model based on the value function of GAN. This may further improve the NCE results.

4 Experiments

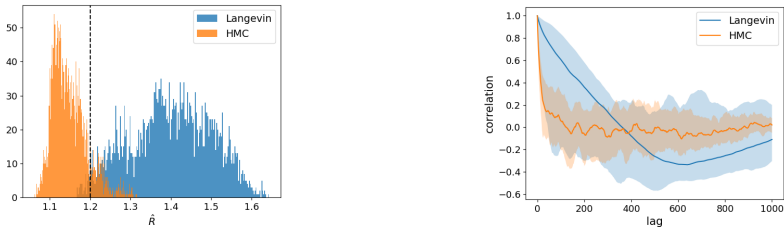
In the subsequent empirical evaluations, we shall address the following questions:

- (1) Is the mixing of HMC with neural transport, both qualitatively and quantitatively, apparent?
- (2) Does the exponential tilting with correction term $f_\theta(x)$ improve the quality of synthesis?
- (3) In the latent space, does smooth interpolation remain feasible?
- (4) In terms of ablation, what is the effect of amount of parameters α for flow-based q_α ?
- (5) Is discriminative learning in the form of NCE an efficient alternative learning method?

4.1 Mixing

Gelman-Rubin. The Gelman-Rubin statistic [15, 7] measures the convergence of Markov chains to the target distribution. It is based on the notion that if multiple chains have converged, by definition, they should appear “similar” to one another, else, one or more chains have failed to converge. Specifically, the diagnostic recruits an analysis of variance to assess the difference between the between-chain and within-chain variances.

Let p denote the target distribution with mean $\mu \in \mathcal{R}$ and variance $\sigma^2 < \infty$. [15] designs two estimators of σ^2 and compares the square root of their ratio to 1. Let $X = \{X_{ij}, i = 1, \dots, m, j = 1, \dots, n\}$ denote m Markov chains of length n . Let $s_w^2 = \frac{1}{m} \sum_{j=1}^m \left[\frac{1}{n-1} \sum_{i=1}^n (X_{ij} - \bar{X}_{.j})^2 \right]$ be the within-chain variance. The quantity s_w^2 underestimates σ^2 due to positive correlation in the Markov chain. Let $\hat{\sigma}^2 = \frac{n-1}{n} s_w^2 + \frac{s_b^2}{n}$ be a mixture of within-chain variance s_w^2 and between-chain variance $s_b^2 = \frac{n}{m-1} \sum_{j=1}^m (\bar{X}_{.j} - \bar{X}_{..})^2$. The quantity $\hat{\sigma}^2$ will overestimate σ^2 , if an over-dispersed initial distribution for the Markov chains was used [15]. That is, s_w^2 underestimates while $\hat{\sigma}^2$ overestimates σ^2 . Both estimators are consistent for σ^2 as $n \rightarrow \infty$ [55]. In light of this, the Gelman-Rubin statistic monitors convergence as the ratio $\hat{R} = \sqrt{\frac{\hat{\sigma}^2}{s_w^2}}$. If all chains converge to p , then as $n \rightarrow \infty$, $\hat{R} \rightarrow 1$. Before that, $\hat{R} > 1$. The heuristics $\hat{R} < 1.2$ indicates approximate convergence [7]. Figure 2a depicts \hat{R} for $m = 64$ chains over $n = 2,000$ steps with a burn-in time of 400 steps. The mean \hat{R} value is 1.13, which we treat as approximative convergence to the target distribution.



(a) Gelman-Rubin statistic for convergence of multiple long-run Markov chains where $\hat{R} < 1.2$ indicates approximative convergence.

(b) Auto-correlation of a single long-run Markov chain over time lag Δt with mean depicted as line and min/max as bands.

Figure 2: Diagnostics for the mixing of MCMC chains with $n = 2,000$ steps and target $p(z)$.



Figure 3: A single long-run Markov Chain with $n = 2,000$ steps depicted in 5 steps intervals sampled by Hamiltonian neural transport. *Left:* SVHN ($32 \times 32 \times 3$). *Right:* CelebA ($64 \times 64 \times 3$).

Auto-Correlation. MCMC sampling leads to autocorrelated samples due to the inherent Markovian dependence structure. The Δt (sample) auto-correlation is the correlation between samples Δt steps apart in time. Figure 2b shows auto-correlation against increasing time lag Δt . While the auto-correlation of Hamiltonian Markov chains with neural transport vanishes within $\Delta t = 200$ steps, the over-damped Langevin sampler requires $\Delta t > 1,000$ steps. This finding for single long-run Markov chain is consistent with the Gelman-Rubin statistic assessing multiple Markov chains.

Visual Inspection. Assume a Markov chain is run for a large numbers of steps $n = 2,000$ with a Hamiltonian neural transport. Then, we pull back Markov chains into data space and visualize the long run trajectory in Figure 3 with p_θ learned on the SVHN ($32 \times 32 \times 3$) [45] dataset and CelebA ($64 \times 64 \times 3$) [42] dataset. We observe the Markov chain is traversing between local modes, which we consider a weak indication of mixing. Figure 4 contrasts the Markov chain that samples the EBM learned with short-run MCMC [47], which does not mix, against our method in which the pulled back chain mixes freely.



Figure 4: Long-run Markov chains for learned models without and with mixing. *Top:* Chains trapped in an over-saturated local mode. Model learned by short-run MCMC [47] without mixing. *Bottom:* Chain is freely traversing local modes. Model learned by Hamiltonian neural transport with mixing.

4.2 Synthesis

We evaluate the quality of synthesis on four datasets which include MNIST ($28 \times 28 \times 1$) [41], SVHN ($32 \times 32 \times 3$) [45], CelebA ($64 \times 64 \times 3$) [42], and, CIFAR-10 ($32 \times 32 \times 3$) [33]. The qualitative results are depicted in Figure 6 which contrast generated samples from Glow q_α against long-run Markov chains by Hamiltonian neural transport. Table 1 compares the Fréchet Inception Distance (FID) [21] with Inception v3 classifier [51] on 50,000 generated examples. Both, qualitatively and quantitatively speaking, we observe a significant improvement in quality of synthesis with exponentially tilting of the reference distribution q_α by the correction f_θ .



(a) Samples drawn from flow q_α by ancestral sampling.

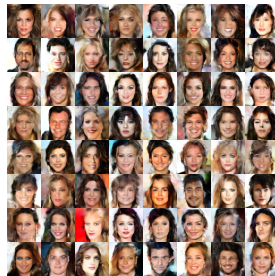


(b) Samples drawn from p_θ by Hamiltonian neural transport.

Figure 5: Generated samples on SVHN ($32 \times 32 \times 3$).



(a) Samples drawn from flow q_α by ancestral sampling.



(b) Samples drawn from p_θ by Hamiltonian neural transport.

Figure 6: Generated samples on CelebA ($64 \times 64 \times 3$).

Table 1: FID scores for generated examples.

Method	MNIST	SVHN	CelebA	CIFAR-10
VAE [30]	32.86	49.72	48.27	106.37
ABP [20]	39.12	48.65	51.92	114.13
Glow (MLE) [31]	66.04	94.23	59.35	90.08
NCE-EBM (Ours)	36.52	79.84	51.73	—
NT-EBM (Ours)	21.32	48.01	46.38	78.12

4.3 Interpolation

Interpolation allows us to appraise the smoothness of the latent space. In particular, two samples z_1 and z_2 are drawn from the prior distribution q_0 . We may spherically interpolate between them in z -space and then push forward into data space to assess q_α . To evaluate the tilted model $p_\theta(z)$, we run a magnetized form of the over-damped Langevin equation for which we alter negative energy $U(z) = f_\theta(g_\alpha(z)) + \log q_0(z)$ to $U_\gamma(z) = U(z) - \gamma \|z - z^*\|_2$ with magnetization constant γ [22]. Note, $\frac{d}{dz} \|z\|_2 = z/\|z\|_2$, thus, the magnetization term introduces a vector field pointing with uniform strength γ towards z^* . The resulting Langevin equation is $dz(t) = \left(\Delta U(z(t)) + \gamma \frac{z(t) - z^*}{\|z(t) - z^*\|_2} \right) dt + \sqrt{2} dW(t)$ with Wiener process $W(t)$. To find a low energy path from z_1 towards z_2 , we set $z^* = z_2$, $z = z_1$ and perform $n = 1,000$ steps of the discretized, magnetized Langevin equation with small γ . Figure 7 depicts the low-energy path in data-space and energy $U(z)$ over time. The qualitatively smooth interpolation and narrow energy spectrum indicate that a Langevin dynamics in latent space (with small magnetization) is able to traverse two arbitrary local modes, thus, substantiating our claim that the underlying geometry is amenable to mixing.

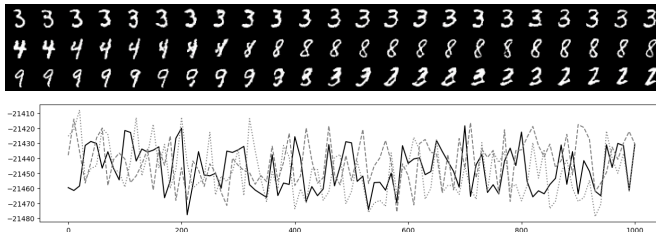


Figure 7: Low energy path between z_1 and z_2 by magnetized Langevin dynamics over $n = 1,000$ steps on MNIST ($28 \times 28 \times 1$). *Top*: Trajectory in data-space. *Bottom*: Energy profile over time.

4.4 Ablation

We investigate the influence of the number of parameters α of flow-based q_α on the quality of synthesis. Specifically, we show (1) the threshold of a “large” q_α learned by MLE outperforming NT with a “small” tilted q_α , and, (2) the minimal size of q_α which allows for the learning by our method. Our method with a “medium” sized backbone significantly outperforms the “largest” Glow baseline.

Table 2: FID scores for generated examples for Glow q_α with varying sizes of parameters α on SVHN ($32 \times 32 \times 3$). Small: $depth = 4$, $width = 128$, Medium: $depth = 8$, $width = 128$. Large: $depth = 16$, $width = 256$, Largest: $depth = 32$, $width = 512$.

Method	Small	Medium	Large	Largest
Glow (MLE) [31]	110.55	94.34	89.31	86.18
NT-EBM (Ours)	74.77	48.01	43.82	—

4.5 Noise Contrastive Estimation

Noise Contrastive Estimation (NCE) is an efficient alternative to our neural transport learning method. We wish to learn the correction f_θ according to (10) while sampling from the learned model with neural transport MCMC. Table 1 compares the learned models with both learning methods. The long-run MCMC chains in models learned by NCE are conducive to mixing and remain of high visual quality. See Appendix 6.6. We leave improvements to this method to future investigations.

5 Conclusion

This paper proposes to learn EBM as a correction or exponential tilting of a flow-based model, so that neural transport MCMC sampling in the latent space of the flow-based model can mix well and traverse the modes in the data space.

Energy-based correction of a more tractable backbone model is a general modeling strategy that goes beyond correcting the flow-based model. Consider latent EBM such as Boltzmann machine [1], which is an undirected graphical model with a simple energy function defined on both the observed variables and multiple layers of latent variables. Instead of learning a latent EBM from scratch, we may learn a latent EBM as a correction of a top-down generation model such as the one in the Helmholtz machine [23], to correct for conditional independence assumptions in the top-down model. We shall investigate this problem in future work.

Acknowledgments

The work is supported by DARPA XAI project N66001-17-2-4029; ARO project W911NF1810296; and ONR MURI project N00014-16-1-2007; and XSEDE grant ASC170063. We thank Matthew D. Hoffman, Diederik P. Kingma, Alexander A. Alemi, and Will Grathwohl for helpful discussions.

References

- [1] David H. Ackley, Geoffrey E. Hinton, and Terrence J. Sejnowski. A learning algorithm for boltzmann machines. *Cognitive Science*, 9(1):147–169, 1985.
- [2] Christophe Andrieu and Johannes Thoms. A tutorial on adaptive mcmc. *Statistics and computing*, 18(4):343–373, 2008.
- [3] Jens Behrmann, Will Grathwohl, Ricky TQ Chen, David Duvenaud, and Jörn-Henrik Jacobsen. Invertible residual networks. *arXiv preprint arXiv:1811.00995*, 2018.
- [4] Yoshua Bengio, Grégoire Mesnil, Yann Dauphin, and Salah Rifai. Better mixing via deep representations. In *International conference on machine learning*, pages 552–560, 2013.
- [5] Alexandros Beskos, Natesh Pillai, Gareth Roberts, Jesus-Maria Sanz-Serna, Andrew Stuart, et al. Optimal tuning of the hybrid monte carlo algorithm. *Bernoulli*, 19(5A):1501–1534, 2013.
- [6] Andrew Brock, Jeff Donahue, and Karen Simonyan. Large scale gan training for high fidelity natural image synthesis. *arXiv preprint arXiv:1809.11096*, 2018.
- [7] Stephen P Brooks and Andrew Gelman. General methods for monitoring convergence of iterative simulations. *Journal of computational and graphical statistics*, 7(4):434–455, 1998.
- [8] Ricky TQ Chen, Jens Behrmann, and Jörn-Henrik Jacobsen. Residual flows: Unbiased generative modeling with norm-learned i-resnets.
- [9] Laurent Dinh, David Krueger, and Yoshua Bengio. Nice: Non-linear independent components estimation. *arXiv preprint arXiv:1410.8516*, 2014.
- [10] Laurent Dinh, Jascha Sohl-Dickstein, and Samy Bengio. Density estimation using real nvp. *arXiv preprint arXiv:1605.08803*, 2016.
- [11] Yilun Du and Igor Mordatch. Implicit generation and generalization in energy-based models. *arXiv preprint arXiv:1903.08689*, 2019.
- [12] Chelsea Finn, Paul Christiano, Pieter Abbeel, and Sergey Levine. A connection between generative adversarial networks, inverse reinforcement learning, and energy-based models. *arXiv preprint arXiv:1611.03852*, 2016.

- [13] Ruiqi Gao, Yang Lu, Junpei Zhou, Song-Chun Zhu, and Ying Nian Wu. Learning generative convnets via multi-grid modeling and sampling. In *Proceedings of the IEEE Conference on Computer Vision and Pattern Recognition*, pages 9155–9164, 2018.
- [14] Ruiqi Gao, Erik Nijkamp, Diederik P Kingma, Zhen Xu, Andrew M Dai, and Ying Nian Wu. Flow contrastive estimation of energy-based models. *arXiv preprint arXiv:1912.00589*, 2019.
- [15] Andrew Gelman, Donald B Rubin, et al. Inference from iterative simulation using multiple sequences. *Statistical science*, 7(4):457–472, 1992.
- [16] Xavier Glorot and Yoshua Bengio. Understanding the difficulty of training deep feedforward neural networks. In *Proceedings of the thirteenth international conference on artificial intelligence and statistics*, pages 249–256, 2010.
- [17] Ian Goodfellow, Jean Pouget-Abadie, Mehdi Mirza, Bing Xu, David Warde-Farley, Sherjil Ozair, Aaron Courville, and Yoshua Bengio. Generative adversarial nets. In *Advances in neural information processing systems*, pages 2672–2680, 2014.
- [18] Will Grathwohl, Ricky TQ Chen, Jesse Bettencourt, Ilya Sutskever, and David Duvenaud. Fjord: Free-form continuous dynamics for scalable reversible generative models. *arXiv preprint arXiv:1810.01367*, 2018.
- [19] Michael Gutmann and Aapo Hyvärinen. Noise-contrastive estimation: A new estimation principle for unnormalized statistical models. In *Proceedings of the Thirteenth International Conference on Artificial Intelligence and Statistics*, pages 297–304, 2010.
- [20] Tian Han, Yang Lu, Song-Chun Zhu, and Ying Nian Wu. Alternating back-propagation for generator network. In *Proceedings of the Thirty-First AAAI Conference on Artificial Intelligence, February 4-9, 2017, San Francisco, California, USA.*, pages 1976–1984, 2017.
- [21] Martin Heusel, Hubert Ramsauer, Thomas Unterthiner, Bernhard Nessler, and Sepp Hochreiter. Gans trained by a two time-scale update rule converge to a local nash equilibrium. In *Advances in Neural Information Processing Systems*, pages 6626–6637, 2017.
- [22] Mitch Hill, Erik Nijkamp, and Song-Chun Zhu. Building a telescope to look into high-dimensional image spaces. *Quarterly of Applied Mathematics*, 77(2):269–321, 2019.
- [23] Geoffrey E Hinton, Peter Dayan, Brendan J Frey, and Radford M Neal. The "wake-sleep" algorithm for unsupervised neural networks. *Science*, 268(5214):1158–1161, 1995.
- [24] Matthew Hoffman, Pavel Soutsov, Joshua V Dillon, Ian Langmore, Dustin Tran, and Srinivas Vasudevan. Neutra-lizing bad geometry in hamiltonian monte carlo using neural transport. *arXiv preprint arXiv:1903.03704*, 2019.
- [25] Long Jin, Justin Lazarow, and Zhuowen Tu. Introspective classification with convolutional nets. In *Advances in Neural Information Processing Systems*, pages 823–833, 2017.
- [26] Ilyes Khemakhem, Diederik P Kingma, and Aapo Hyvärinen. Variational autoencoders and nonlinear ica: A unifying framework. *arXiv preprint arXiv:1907.04809*, 2019.
- [27] Taesup Kim and Yoshua Bengio. Deep directed generative models with energy-based probability estimation. *arXiv preprint arXiv:1606.03439*, 2016.
- [28] Diederik Kingma and Max Welling. Efficient gradient-based inference through transformations between bayes nets and neural nets. In *International Conference on Machine Learning*, pages 1782–1790, 2014.
- [29] Diederik P. Kingma and Jimmy Ba. Adam: A method for stochastic optimization. In *3rd International Conference on Learning Representations, ICLR 2015, San Diego, CA, USA, May 7-9, 2015, Conference Track Proceedings*, 2015.
- [30] Diederik P Kingma and Max Welling. Auto-encoding variational bayes. *arXiv preprint arXiv:1312.6114*, 2013.
- [31] Durk P Kingma and Prafulla Dhariwal. Glow: Generative flow with invertible 1x1 convolutions. In *Advances in Neural Information Processing Systems*, pages 10215–10224, 2018.
- [32] Durk P Kingma, Tim Salimans, Rafal Jozefowicz, Xi Chen, Ilya Sutskever, and Max Welling. Improved variational inference with inverse autoregressive flow. In *Advances in neural information processing systems*, pages 4743–4751, 2016.
- [33] Alex Krizhevsky, Vinod Nair, and Geoffrey Hinton. Cifar-10 (canadian institute for advanced research).

- [34] Alex Krizhevsky, Ilya Sutskever, and Geoffrey E Hinton. Imagenet classification with deep convolutional neural networks. In *Advances in neural information processing systems*, pages 1097–1105, 2012.
- [35] Manoj Kumar, Mohammad Babaeizadeh, Dumitru Erhan, Chelsea Finn, Sergey Levine, Laurent Dinh, and Durk Kingma. Videoflow: A flow-based generative model for video. *arXiv preprint arXiv:1903.01434*, 2019.
- [36] Rithesh Kumar, Anirudh Goyal, Aaron Courville, and Yoshua Bengio. Maximum entropy generators for energy-based models. *arXiv preprint arXiv:1901.08508*, 2019.
- [37] Paul Langevin. *On the theory of Brownian motion*. 1908.
- [38] Justin Lazarow, Long Jin, and Zhuowen Tu. Introspective neural networks for generative modeling. In *Proceedings of the IEEE International Conference on Computer Vision*, pages 2774–2783, 2017.
- [39] Yann LeCun, Léon Bottou, Yoshua Bengio, Patrick Haffner, et al. Gradient-based learning applied to document recognition. *Proceedings of the IEEE*, 86(11):2278–2324, 1998.
- [40] Yann LeCun, Sumit Chopra, Raia Hadsell, M Ranzato, and F Huang. A tutorial on energy-based learning. *Predicting structured data*, 1(0), 2006.
- [41] Yann LeCun, Corinna Cortes, and CJ Burges. Mnist handwritten digit database. *ATT Labs [Online]*. Available: <http://yann.lecun.com/exdb/mnist>, 2, 2010.
- [42] Ziwei Liu, Ping Luo, Xiaogang Wang, and Xiaoou Tang. Deep learning face attributes in the wild. In *Proceedings of International Conference on Computer Vision (ICCV)*, 2015.
- [43] Oren Mangoubi and Aaron Smith. Rapid mixing of hamiltonian monte carlo on strongly log-concave distributions. *arXiv preprint arXiv:1708.07114*, 2017.
- [44] Radford M Neal. MCMC using hamiltonian dynamics. *Handbook of Markov Chain Monte Carlo*, 2, 2011.
- [45] Yuval Netzer, Tao Wang, Adam Coates, Alessandro Bissacco, Bo Wu, and Andrew Y Ng. Reading digits in natural images with unsupervised feature learning. 2011.
- [46] Jiquan Ngiam, Zhenghao Chen, Pang W Koh, and Andrew Y Ng. Learning deep energy models. In *Proceedings of the 28th international conference on machine learning (ICML-11)*, pages 1105–1112, 2011.
- [47] Erik Nijkamp, Song-Chun Zhu, and Ying Nian Wu. On learning non-convergent short-run mcmc toward energy-based model. *arXiv preprint arXiv:1904.09770*, 2019.
- [48] Prajit Ramachandran, Barret Zoph, and Quoc V Le. Searching for activation functions. *arXiv preprint arXiv:1710.05941*, 2017.
- [49] Danilo Jimenez Rezende and Shakir Mohamed. Variational inference with normalizing flows. *arXiv preprint arXiv:1505.05770*, 2015.
- [50] Ronald Rosenfeld, Stanley F Chen, and Xiaojin Zhu. Whole-sentence exponential language models: a vehicle for linguistic-statistical integration. *Computer Speech & Language*, 15(1):55–73, 2001.
- [51] Christian Szegedy, Vincent Vanhoucke, Sergey Ioffe, Jon Shlens, and Zbigniew Wojna. Rethinking the inception architecture for computer vision. In *Proceedings of the IEEE conference on computer vision and pattern recognition*, pages 2818–2826, 2016.
- [52] Tijmen Tieleman. Training restricted boltzmann machines using approximations to the likelihood gradient. In *Proceedings of the 25th international conference on Machine learning*, pages 1064–1071, 2008.
- [53] Dustin Tran, Keyon Vafa, Kumar Krishna Agrawal, Laurent Dinh, and Ben Poole. Discrete flows: Invertible generative models of discrete data. *arXiv preprint arXiv:1905.10347*, 2019.
- [54] Zhuowen Tu. Learning generative models via discriminative approaches. In *2007 IEEE Conference on Computer Vision and Pattern Recognition*, pages 1–8. IEEE, 2007.
- [55] Dootika Vats and Christina Knudson. Revisiting the gelman-rubin diagnostic. *arXiv preprint arXiv:1812.09384*, 2018.

- [56] Bin Wang and Zhijian Ou. Learning neural trans-dimensional random field language models with noise-contrastive estimation. In *2018 IEEE International Conference on Acoustics, Speech and Signal Processing (ICASSP)*, pages 6134–6138. IEEE, 2018.
- [57] Jianwen Xie, Yang Lu, Song-Chun Zhu, and Yingnian Wu. A theory of generative convnet. In *International Conference on Machine Learning*, pages 2635–2644, 2016.
- [58] Junbo Zhao, Michael Mathieu, and Yann LeCun. Energy-based generative adversarial network. *arXiv preprint arXiv:1609.03126*, 2016.

6 Appendix

6.1 Change of variable

Under the invertible transformation $x = g(z)$, let $p(z)$ be the density of z , and $p(x)$ be the density of x . Let D_z be an infinitesimal neighborhood around z , and let D_x be an infinitesimal neighborhood around x , so that g maps z to x , and maps D_z to D_x . Then

$$\Pr(D_z) = \Pr(D_x). \quad (11)$$

$\Pr(D_z) = p(z)|D_z| + o(|D_z|)$, and $\Pr(D_x) = p(x)|D_x| + o(|D_x|)$, where $|D_z|$ and $|D_x|$ are the volumes of D_z and D_x respectively. Thus we have

$$p(z)|D_z| = p(x)|D_x|, \quad (12)$$

where we ignore $o(|D_z|)$ and $o(|D_x|)$ terms. This is the meaning of

$$p(z)dz = p(x)dx, \quad (13)$$

where $|D_x|/|D_z|$ or dx/dz is the determinant of the Jacobian of g .

Equation (13) is a convenient starting point for deriving densities under change of variable.

6.2 Energy-based correction and change of variable for generator model

The generator model is of the form $z \sim N(0, I_d)$, and $x = g_\alpha(z) + \epsilon$, $\epsilon \sim N(0, \sigma^2 I_D)$, where D is the dimensionality of x , and $d \ll D$ is the dimensionality of the latent vector. Unlike the flow-based model, the marginal distribution of x involves intractable integral.

We shall study exponential tilting of generator model using the simple equation (13) for change of variable. To that end, we let $\tilde{z} = (z, \epsilon)$, and let $\tilde{x} = (z, x)$. Then

$$\tilde{x} = (z, x) = G_\alpha(\tilde{z}) = G_\alpha(z, \epsilon) = (z, g_\alpha(z) + \epsilon). \quad (14)$$

Let $q_0(\tilde{z})$ be the Gaussian white noise distribution of \tilde{z} under the generator model. Let $q_\alpha(\tilde{x})$ be the distribution of \tilde{x} under the generator model. Consider the change of variable between \tilde{z} and \tilde{x} . In parallel to equation (13), we have

$$q_0(\tilde{z})d\tilde{z} = q_\alpha(\tilde{x})d\tilde{x}. \quad (15)$$

The marginal distribution $q_\alpha(x) = \int q_\alpha(\tilde{x})dz = \int q_\alpha(z, x)dz$, which is intractable.

Suppose we exponentially tilt $q_\alpha(\tilde{x})$ to

$$p_\theta(\tilde{x}) = \frac{1}{Z(\theta)} \exp(f_\theta(\tilde{x}))q_\alpha(\tilde{x}). \quad (16)$$

Again this can be translated into the space of \tilde{z} so that under $p_\theta(\tilde{x})$,

$$p(\tilde{z})d\tilde{z} = p_\theta(\tilde{x})d\tilde{x}. \quad (17)$$

Combining equations (15), (16), and (17), we have

$$p(\tilde{z}) = \frac{1}{Z(\theta)} \exp(f_\theta(G_\alpha(\tilde{z})))q_0(\tilde{z}), \quad (18)$$

that is, under the tilted model $p_\theta(\tilde{x})$,

$$p(z, \epsilon) = \frac{1}{Z(\theta)} \exp(f_\theta(z, g_\alpha(z) + \epsilon))q_0(z, \epsilon). \quad (19)$$

For $p(z, \epsilon)$, the marginal distribution $p(z)$ cannot be obtained in closed form, in particular, for gradient-based sampling, we need to compute

$$\nabla_z \log p(z) = \frac{1}{p(z)} \int \nabla_z p(z, \epsilon) d\epsilon \quad (20)$$

$$= \int [\nabla_z \log p(z, \epsilon)] \frac{p(z, \epsilon)}{p(z)} d\epsilon \quad (21)$$

$$= \mathbb{E}_{p(\epsilon|z)}[\nabla_z \log p(z, \epsilon)]. \quad (22)$$

That is, there is an inner loop for approximating $\mathbb{E}_{p(\epsilon|z)}$. This is less convenient than the flow-based model.

6.3 Model architectures

For Glow model q_α , we follow the setting of [31] with $n_bits_x = 8$, $flow_permutation = 2$, $flow_coupling = 0$.

For the EBM model f_θ , we use the following Conv-Net structure.

We use the following notation. Convolutional operation $conv(n)$ with n output feature maps and bias term. We recruit $LipSwish(x) = Swish(x)/1.1$ [8] nonlinearity where $Swish(x) = x * sigmoid(x)$ [48] as activation function. We set $n_f \in \{32, 64\}$.

Specifically, we set use the following hyper-parameters:

1. **MNIST**: For Glow, $n_levels = 3$, $depth = 8$, $width = 128$. For EBM, $n_f = 32$.
2. **SVHN**: For Glow, $n_levels = 3$, $depth = 8$, $width = 128$. For EBM, $n_f = 32$.
3. **CelebA**: For Glow, $n_levels = 3$, $depth = 16$, $width = 256$. For EBM, $n_f = 32$.
4. **CIFAR-10**: For Glow, $n_levels = 3$, $depth = 16$, $width = 512$. For EBM, $n_f = 32$.

Energy-based Model ($32 \times 32 \times 3$)		
Layers	In-Out Size	Stride
Input	$32 \times 32 \times 3$	
3×3 conv(n_f), <i>LipSwish</i>	$32 \times 32 \times n_f$	1
4×4 conv($2 * n_f$), <i>LipSwish</i>	$16 \times 16 \times (2 * n_f)$	2
4×4 conv($4 * n_f$), <i>LipSwish</i>	$8 \times 8 \times (4 * n_f)$	2
4×4 conv($4 * n_f$), <i>LipSwish</i>	$4 \times 4 \times (4 * n_f)$	2
4×4 conv(1)	$1 \times 1 \times 1$	1

Table 3: Network structures for EBM with data-space ($32 \times 32 \times 3$).

Energy-based Model ($64 \times 64 \times 3$)		
Layers	In-Out Size	Stride
Input	$64 \times 64 \times 3$	
3×3 conv(n_f), <i>LipSwish</i>	$64 \times 64 \times n_f$	1
4×4 conv($2 * n_f$), <i>LipSwish</i>	$32 \times 32 \times (2 * n_f)$	2
4×4 conv($4 * n_f$), <i>LipSwish</i>	$16 \times 16 \times (4 * n_f)$	2
4×4 conv($8 * n_f$), <i>LipSwish</i>	$8 \times 8 \times (8 * n_f)$	2
4×4 conv($8 * n_f$), <i>LipSwish</i>	$4 \times 4 \times (8 * n_f)$	2
4×4 conv(1)	$1 \times 1 \times 1$	1

Table 4: Network structures for EBM with data-space ($64 \times 64 \times 3$).

6.4 Training

Data. The training image dataset are resized and scaled to $[-1, 1]$. We use 60,000, 70,000, 30,000, 50,000 observed examples for MNIST ($28 \times 28 \times 1$), SVHN ($32 \times 32 \times 3$), CelebA ($64 \times 64 \times 3$), and CIFAR-10 ($32 \times 32 \times 3$), respectively.

Optimization. The network parameters are initialized with Xavier [16] and optimized using Adam [29] with $(\beta_1, \beta_2) = (0.99, 0.999)$. For NT-EBM, the learning rates used are $5e-5$, $5e-5$, $1e-5$, $5e-5$ for MNIST, SVHN, CelebA, CIFAR-10, respectively and a batch-size of 64 examples. For NCE-EBM, the learning rates used are $1e-5$, $1e-5$, $1e-5$ for MNIST, SVHN, and CelebA, respectively, and a batch-size of 128 examples. For NT-EBM, in training the maximum number of

parameter θ updates was 40,000. For NCE-EBM, in training the maximum number of parameter θ updates was 80,000.

HMC. We run Hamiltonian Monte Carlo (HMC) with persistent chains [52] initialized from q_α and 20 steps of MCMC and 3 leapfrog integrator steps per update of parameters of θ . The initial discretization step-size 0.15 with a simple adaptive policy multiplicatively increases or decreasing the step-size of the inner kernel based on the value of the Metropolis-Hastings acceptance rate [2]. The target acceptance-rate is set to 0.651 [5]. Figure 8 depicts the MH acceptance-rate and adaptive step-size over time.

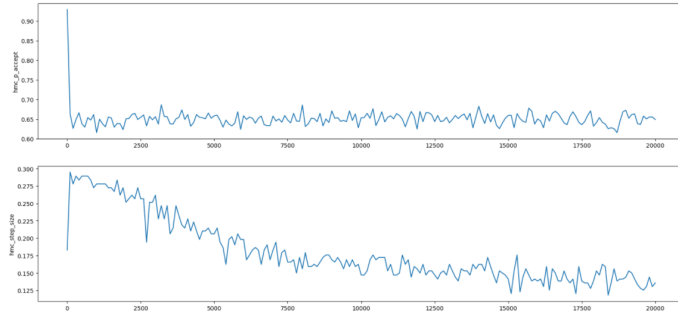


Figure 8: Metropolis-Hastings acceptance rate (top) and adaptive step-size (bottom) over time.

FID. The Fréchet Inception Distance (FID) [21] with Inception v3 classifier [51] was computed on 50,000 generated examples with 50,000 observed examples as reference.

6.5 Synthesis

Figure 9 depicts samples from pre-trained flow q_α and samples from p_θ learned by neural transport MCMC for the dataset CIFAR-10 ($32 \times 32 \times 3$).



(a) Samples drawn from flow q_α by ancestral sampling.

(b) Samples drawn from p_θ by Hamiltonian neural transport.

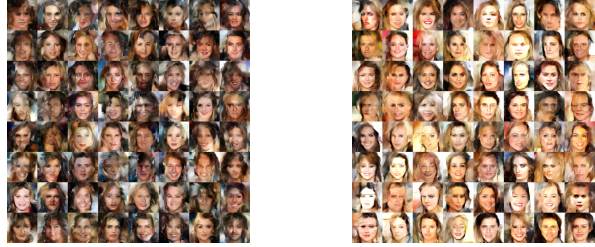
Figure 9: Generated samples from a model learned by NT-EBM on CIFAR-10 ($32 \times 32 \times 3$).

6.6 Noise contrastive estimation

For numerical stability, the noise contrastive estimation objective is rewritten in the equivalent form using `tf.math.log_sigmoid()` and `tf.math.softplus()`.

Figure 10 depicts samples from q_α (left) and samples from p_θ learned by our NCE algorithm for which sampling is performed using Hamiltonian neural transport (right) for the dataset CelebA ($64 \times 64 \times 3$).

We learn f_θ with our NCE-EBM algorithm on the SVHN ($32 \times 32 \times 3$) [45] dataset and investigate the possibility of sampling from the learned model by Hamiltonian neural transport. Assume a Markov chain is run for a large numbers of steps $n = 2,000$ with a Hamiltonian neural transport. Then, we pull back Markov chains into data space and visualize the long run trajectory in Figure 11 with p_θ . Note, the long-run Markov chains synthesizes realistic images with high diversity.



(a) Samples drawn from flow q_α by ancestral sampling. (b) Samples drawn from p_θ by Hamiltonian neural transport.

Figure 10: Generated samples from a model learned by NCE on CelebA ($64 \times 64 \times 3$).

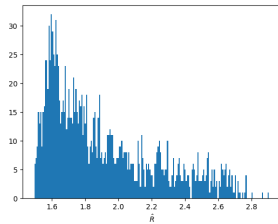


Figure 11: A single long-run Markov Chain with $n = 2,000$ steps depicted in 5 steps intervals sampled by Hamiltonian neural transport for a model learned by NCE on SVHN ($32 \times 32 \times 3$).

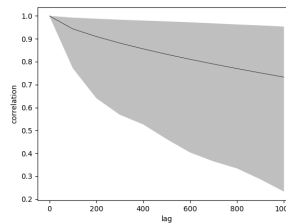
Notice that NCE is the discriminator side of GAN. Similar to GAN, we can also improve the flow-based model based on the value function of GAN. This may further improve the NCE results.

6.7 Sampling in data space

In Section 4.1, we analyze the quality of mixing with multiple Markov chains based on the Gelman-Rubin statistic \hat{R} . Recall, $\hat{R} < 1.2$ is considered approximate convergence [7]. We concluded sampling with Hamiltonian neural transport exhibits a strong indication of mixing. In Figure 12, we contrast this result with HMC sampling in data space with unfavorable diagnostics of mixing.



(a) Gelman-Rubin statistic for convergence of multiple long-run Markov chains where $\hat{R} < 1.2$ indicates approximative convergence.



(b) Auto-correlation of a single long-run Markov chain over time lag Δt with mean depicted as line and min/max as bands.

Figure 12: Diagnostics for the mixing of MCMC chains with $n = 2,000$ steps in data space.